

GW190412: measuring a black-hole recoil direction through higher-order gravitational-wave modes

Juan Calderón Bustillo,^{1,2} Samson H. W. Leong,² and Koustav Chandra³

¹*Instituto Galego de Física de Altas Enerxías, Universidade de Santiago de Compostela, 15782 Santiago de Compostela, Galicia, Spain*

²*Department of Physics, The Chinese University of Hong Kong, Shatin, N.T., Hong Kong*

³*Department of Physics, Indian Institute of Technology Bombay, Powai, Mumbai, Maharashtra 400076, India*

General relativity predicts that gravitational waves (GWs) carry linear momentum. Consequently, the remnant black hole of a black-hole merger can inherit a recoil velocity or “kick” of crucial implications in, e.g, black-hole formation scenarios. While the kick magnitude is determined by the mass ratio and spins of the source, estimating its direction requires a measurement of the *two orientation angles* of the source. While the orbital inclination angle is commonly reported in GW observations, the azimuthal one has been to date ignored. We show how the presence of more than one GW emission mode allows constraining this angle and, consequently, determines the kick direction in a real GW event. We analyse the GW190412 signal, which contains higher-order modes, with a numerical-relativity surrogate waveform model for black-hole mergers. We find that while GW190412 is barely informative about the kick magnitude, we can constrain its direction. This forms angles $\theta_{KL}^{100M} = 28_{-11}^{+23}$ deg with the orbital angular momentum defined at a reference time $t_{\text{ref}} = -100 M$ before merger (being preferentially kicked upwards), $\theta_{KN} = 37_{-12}^{+15}$ deg with the line-of-sight and $\phi_{KN}^{100M} = 46_{-41}^{+32}$ deg with the projection of the latter onto the former, all at the 68% credible level. We briefly discuss the potential application of this type of measurement for multi-messenger observations of black-hole mergers occurring in Active Galactic Nuclei.

I. INTRODUCTION

Gravitational waves (GWs) carry linear momentum away from their sources [1] and asymmetric black-hole (BBH) mergers emit GWs in an anisotropic way. This causes a net emission of linear momentum that makes the final black hole (BH) acquire a recoil velocity [2–10], or kick, that in the most extreme cases can reach $\mathcal{O}(1000)$ km/s [9, 11–17]. Such speeds can expel the remnant BH from their host environments preventing them from taking part in subsequent mergers and, therefore, from contributing to hierarchical BH formation mechanisms [18]. This has crucial astrophysical consequences as, e.g., such scenarios shall explain the formation of supermassive BHs [19–21]. Due to its paramount importance in BH formation, much work has been devoted towards estimating the kick magnitude of the remnant BHs of the GW events observed by Advanced LIGO [22] and Advanced Virgo [23] [24–26]. The kick magnitude is determined by the mass ratio and spins of the merging BHs [9, 11–16], with the spin relative orientations playing a particularly important role. Estimating these, however, is a difficult task [27, 28]. Consequently, only two of the $\sim \mathcal{O}(100)$ events detected to date [29–37], namely GW190814 [38] and GW200129_065458 [25] (GW200129 hereafter), allow for an informative estimation of the recoil magnitude. Estimating the recoil direction requires, in contrast, an estimate of the two angles characterising the Earth’s location on the binary’s sky, which can be conversely understood as the BBH orientation w.r.t. the observer. We can access such information through the gravitational-wave mode content of the signal, as we outline next.

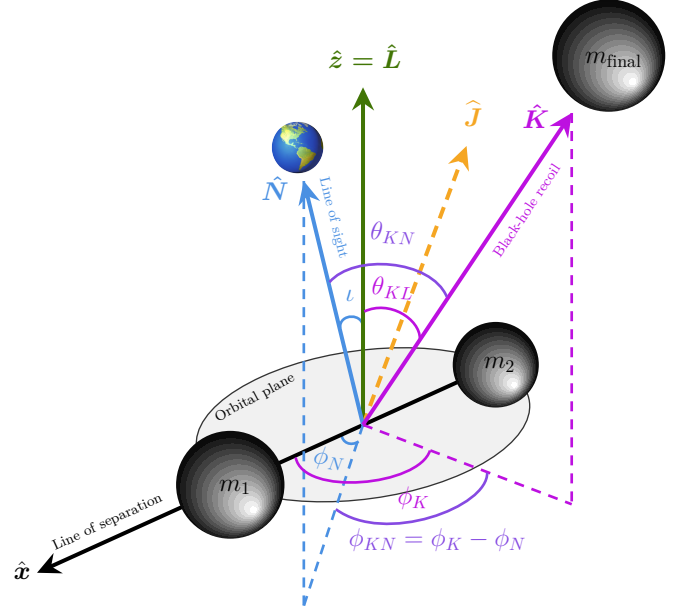


FIG. 1. **Sketch of our black-hole merger reference frame** The polar and azimuthal angles (l, ϕ_N) characterise the orientation of the orbital plane of a black-hole merger or, conversely, the direction of the line-of-sight \hat{N} on its sky. The vector \hat{K} represents the final black-hole recoil (or kick). Its direction on the binary’s sky is characterised by θ_{KL} and ϕ_K . Finally, we characterise its direction with respect to the line-of-sight by the angles θ_{KN} and ϕ_{KN} .

II. METHODS

A. The source frame and the orientation angles

The GW emission from a BBH can be described as a superposition of the several GW modes $h_{\ell,m}$ weighted by spin-2 spherical harmonics $Y_{\ell,m}^{-2}$ as [39, 40]:

$$h_+ - ih_\times = \sum_{\ell,m} Y_{\ell,m}^{-2}(\iota, \phi_N) h_{\ell,m}(\Xi; t). \quad (1)$$

Here, Ξ denotes the intrinsic parameters (masses and spins) of the source. The parameter ι denotes the polar angle formed between the line-of-sight (LOS) and the (instantaneous) orbital angular momentum \mathbf{L} , normal to the orbital plane defined at a given reference time t_{ref} during the BBH evolution. The value $\iota = 0$ denotes a “face-on” observer while $\iota = \pi/2$ denotes an “edge-on” observer located on the orbital plane. The angle ϕ_N denotes the azimuthal angle of the observer, *i.e.*, the angle formed by the projection of the line-of-sight \mathbf{N} onto the orbital plane and some preferential axis $\hat{\mathbf{x}}$ [10] on it, which is commonly chosen¹ as the vector pointing from the lighter to the heavier BH [42].

B. Characterising the kick direction and re-defining the azimuthal angle

Within the above frame, the final BH kick \mathbf{K} can be characterised by its magnitude K and the angles (θ_{KL}, ϕ_K) that it forms with \mathbf{L} and $\hat{\mathbf{x}}$ (See Fig. 1). Using the kick and the LOS, we can compute two more “observer-related” angles: the angle θ_{KN} subtended between them and the angle $\phi_{KN} = \phi_K - \phi_N$ formed by their projections on the orbital plane.

BBHs with spins (anti-)aligned with $\hat{\mathbf{L}}$ display a constantly oriented orbital plane. In this case, although ι is time-independent, ϕ_N clearly depends on t_{ref} . This partly motivates the latter to be systematically treated as a sort of “nuisance” parameter not reported in GW catalogues, commonly referred to as “coalescence phase”. The angle ϕ_{KN} however, provides a time-independent and more astrophysically motivated re-definition of the azimuthal location of the observer [10] which, in the following, we will use to characterise both the source orientation and the kick direction.

Finally, for generically spinning BBHs, spin-orbit coupling causes \mathbf{L} to precess around the total angular momentum \mathbf{J} [43]. This leads to a time-dependent orientation of the orbital plane, ι and ϕ_{KN} . In this situation, it is common to replace the inclination angle ι by the angle θ_{JN} formed between the LOS and the almost-conserved \mathbf{J} . Analogously, we can replace ϕ_N by the angle ϕ_N^J formed between the projections of the LOS and \mathbf{K} onto the plane normal to \mathbf{J} .

C. Reading the kick and orientation angles from gravitational waves: GW200129 and GW190412

The spherical harmonics $Y_{\ell,m}^{-2}(\iota, \phi_N)$ can be decomposed into amplitude and phase terms as $Y_{\ell,m}^{-2}(\iota, \phi_N) = |Y_{\ell,m}^{-2}(\iota)| e^{-im\phi_N}$. This shows that while ι controls the amplitude of each mode, ϕ_N determines the relative phase with which these modes interact, dramatically impacting the morphology, (*i.e.* the frequency content) of the observed signal [44]. Consequently, ϕ_N should be measurable if more than one mode with distinct frequency content is observed in the signal. This, however, requires the observation of either a precessing and/or high-mass ratio BBH with non-zero inclination, which is a challenging task.

First, the BBH emission is vastly dominated by the so-called “quadrupole” modes $(\ell, m) = (2, \pm 2)$, while further modes with $(\ell, m) \neq (2, \pm 2)$, known as higher-order modes (HMs), only reach comparable amplitudes near the merger stages of asymmetric sources. Second, since the face-on(off) emissions are respectively dominated by the $\ell = 2, m = +2(-2)$ modes, only signals emitted at $\iota \neq (0, \pi)$ can have significant HM content. Third, the joint observation of both dominant modes can allow for an estimation of ϕ_N in the case of precessing sources. For non-precessing cases, however, these modes are related by $h_{2,-2} = h_{2,2}^*$. This reduces the impact of ϕ_N in the quadrupole signal to a trivial phase shift [40, 45, 46], preventing its measurement. Therefore, in such cases, we can only obtain information about ϕ_N through the observation of HMs.

In addition, detecting these types of signals is nowadays very challenging. First, signals from highly inclined systems are much weaker than those emitted face-on, reducing the chance of detection. Second, current matched-filter searches only target the quadrupole modes of non-precessing BBHs, dramatically damaging our sensitivity towards HM-rich or precessing signals [45–52].

Despite this, the LVK confidently observed two such signals during its third observing run. First, GW200129 [53] was claimed to show conclusive signatures of precession [54] which, in turn, allowed for an informative estimation of the kick magnitude $K > 698$ km/s [25] and, although not emphasised therein, a characterisation of the kick direction. We note, however, that the interpretation of this signal has been recently

¹ We note that waveform models used within the LIGO–Virgo–KAGRA Collaboration (LVK), that are implemented within the software `lalsuite` [41], use a definition for the azimuthal angle $\phi_N^{\text{LVK}} = \pi/2 - \phi_N$. (See `phiRef` or `Phi` in [42].)

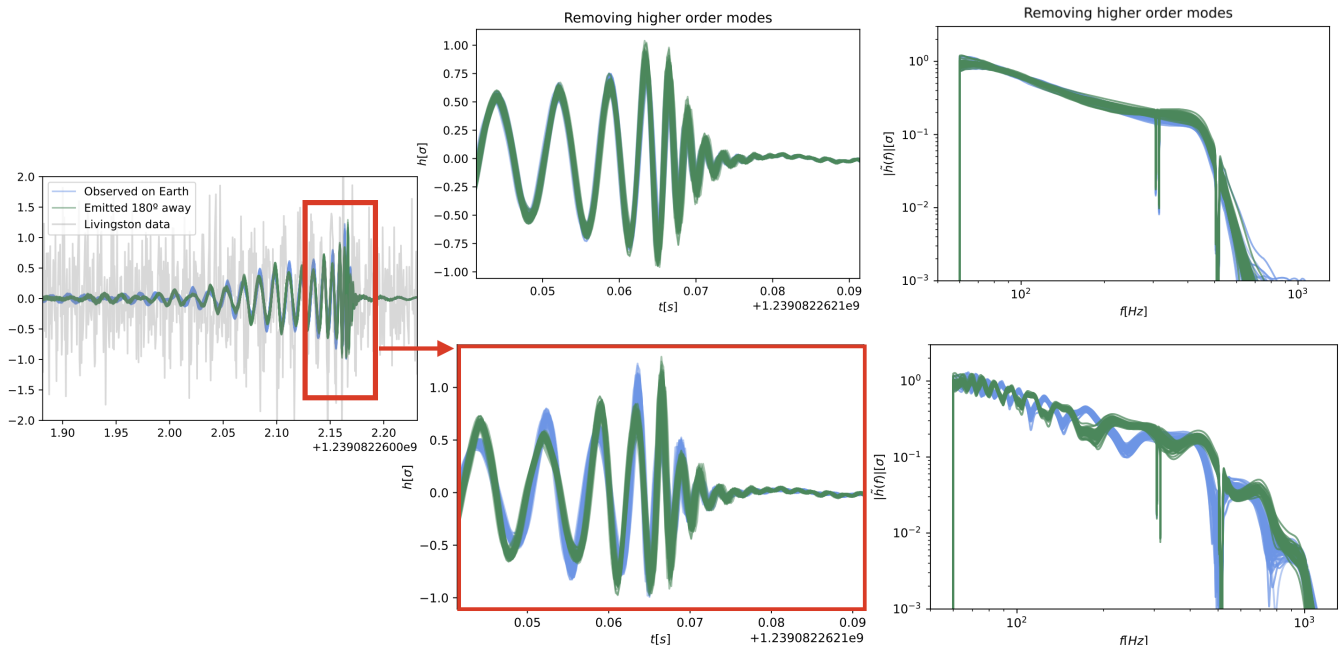


FIG. 2. **GW190412 as observed on Earth and 180 deg away: impact of higher-order modes.** The left panel shows the whitened LIGO Livingston data around GW190412 together with the corresponding top-100 highest likelihood (best fit) waveforms in blue. In green, we also show the signals emitted by the source in the direction opposite to the line-of-sight, which clearly differ. The mid-bottom panel zooms into the late-inspiral and merger region to highlight morphological differences. Finally, the right-bottom panel shows the corresponding Fourier transforms. The top central and right panels show the same as the bottom ones, but restricting the waveforms to only the dominant quadrupole $(2, \pm 2)$ modes. This removes the information about the azimuthal angle, making the two sets of waveforms indistinguishable.

challenged by Payne *et al.* [55], suggesting that the inference of precession may be due to data-quality issues in the Livingston detector. In this situation, we turn our attention to the event GW190412 [56], reported as a BBH which, while showing no signatures of precession, has a mass-ratio $q \simeq 3$ and orbital inclination $\iota \geq 30$ deg at the 90% credible level. Consequently, it was concluded that GW190412 contains measurable HMs [57], making it an optimal candidate for estimating the kick direction.

D. Parameter inference

We perform Bayesian parameter inference on 4 seconds of publicly available data from the two Advanced LIGO and the Advanced Virgo detectors around the time of GW190412, sampled at 2048 Hz, using the software *Parallel Bilby* [58]. We compare GW190412 with the state-of-the-art BBH waveform template model *NRSur7dq4* [59], which includes the impact of orbital precession and HMs.

Our waveform model choice is motivated by two factors. First, unlike the models for precessing BBHs used by the LVK for the analysis of this signal (namely *IMRPhenomXPHM* [60] and *SEOBNRv4PHM* [61–63]),

NRSur7dq4 is directly fitted to generically precessing numerical relativity (NR) simulations. In particular, on the one hand, the first two models reproduce the impact of precession through post-Newtonian approximations that break down near the merger stage [64, 65]. On the other hand, and more crucial for this study, the relative phase of the individual $h_{\ell,m}$ modes of these models is not calibrated to NR during the merger-ringdown stage, which can lead to biased estimations of both the kick magnitude, direction and azimuthal angle [66–68]. Second, the associated model *NRSur7dq4Remnant* [69] provides accurate estimations of the magnitude and direction of the kick given the BBH parameters. As a shortcoming, the limited time length of the waveforms generated by *NRSur7dq4* prevents the analysis of the full signal. We therefore start our analysis at a frequency $f_{\min} = 60$ Hz, instead of the value $f_{\min} = 20$ Hz used by the LVK. We find that despite missing the information in the 20 – 60 Hz band, we obtain parameter estimates with uncertainties comparable to those of the LVK while also obtaining informative posteriors on the kick direction.

We place standard priors on all the 15 BBH parameters and sample the likelihood across the parameter space using the nested sampler *Dynesty* [70] with 4096

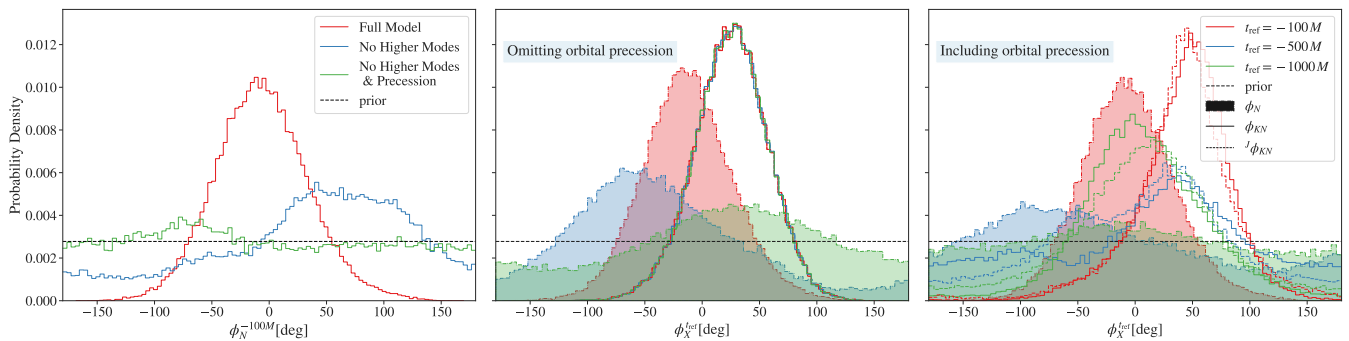


FIG. 3. **Azimuthal angle around GW190412: impact of higher-order modes and precession.** The left panel shows the posterior distributions of the azimuthal location of Earth ϕ_N^{-100M} around GW190412, defined as the angle between the projection of the line-of-sight onto the orbital plane and the line joining the two BHs at a time $t_{\text{ref}} = -100M$ before merger. We show this for analyses including higher modes and precession, ignoring higher modes and ignoring both effects. The filled histograms in the central and rightmost panels show the same quantity, also computed at times $t_{\text{ref}} = -500M$ and $-1000M$. The empty histograms, instead, show the angle formed by the projections of the kick and the line-of-sight on the orbital plane $\phi_{KN}^{t_{\text{ref}}}$ (solid) and the plane normal to the total angular momentum \mathbf{J} (dashed) ${}^J\phi_{KN}^{t_{\text{ref}}}$. In the central panel, we ignore orbital precession in the analysis while in the right panel we include it.

live points. Finally, in order to show that the kick direction characterisation comes from the information encoded in the HMs, we also analyse GW190412 by removing HMs and/or precession from our templates. We report our results as median values together with symmetric 68% credible intervals.

III. RESULTS

A. Visualising GW190412 and the kick impact

The left panel of Fig. 2 shows the whitened data from the Livingston detector at the time of GW190412 (grey) together with the 100 best-fitting templates (blue). In green, we show the corresponding signals observed in the opposite direction around the source, *i.e.*, observed at $(\iota^{\text{Earth}}, \phi_N^{\text{Earth}} + \pi)$. The bottom-central panel shows the last few cycles of these waveforms while the top-central panel shows the same waveforms, but with the HMs removed. While in the first case the two sets of signals clearly differ, therefore enabling measurement of ϕ_N and ϕ_{KN} , these are almost identical when HMs are removed, preventing such measurements. Finally, the rightmost panels show these waveforms in the frequency domain. The bottom panel makes obvious that the two waveforms show very different frequency content as a result of different interactions of the GW modes [10, 44]. Finally, [10] both the central and right bottom panels show that, unlike previously claimed [71], the impact of the kick direction – hence that of speed of the final BH relative to the observer – *is not accounted* by a relative Doppler shift of the signal, but, instead, is encoded in morphological differences arising from the different mode combinations recorded by the

corresponding observers around the source, as shown in [10, 44].

B. Earth’s azimuthal angle ϕ_N around GW190412

The left panel of Fig. 3 shows in red the posterior distribution for ϕ_N inferred when HMs are included in the analysis, estimated at a reference time $t_{\text{ref}} = -100M$ before merger. The prior probability is shown in black. Blue/green posteriors omit HMs and respectively include/omit orbital precession. The omission of HMs yields uninformative posteriors, as expected,² while the inclusion of HMs leads to clearly informative posterior, yielding $\phi_N^{-100M} = -7_{-42}^{+44}$ deg. To highlight the time-dependence of ϕ_N , the filled histograms of the central panel show the posterior for ϕ_N^{-100M} compared to those obtained at $t_{\text{ref}} = -500M$ and $-1000M$ when orbital precession is omitted. The empty histograms, on the other hand, show the angles ϕ_{KN} , computed on the orbital plane, and ${}^J\phi_{KN}$ (solid lines), computed on the plane normal to \mathbf{J} (dashed). As expected, in the absence of precession, these two are coincident and time-independent, providing a clear physical interpretation of the azimuthal angle. Finally, the right panel shows the same quantities as the central one but when precession is included in the analysis. While both ϕ_{KN} and ${}^J\phi_{KN}$ now depend on t_{ref} , we can see that their variability

² We note that when precession is considered, certain information on ϕ_N can be retrieved even if ignoring higher modes. The reason is that while the $(2, \pm 2)$ modes are related by $h_{2,-2} = h_{2,2}^*$ for non-precessing sources, and therefore have identical frequency content, such relation does not hold in general.

is much lower than that of ϕ_N . In all of the following, unless otherwise specified, we quote measurements using $t_{\text{ref}} = -100 M$ following the prescription of [25, 67].

C. The kick of GW190412

Fig. 4 shows, in red, the two-dimensional 68% credible regions for the kick magnitude K and the angles θ_{KN} , θ_{KL}^{-100M} and ϕ_{KN}^{-100M} , together with the corresponding one-dimensional distributions. The prior distributions are shown in grey. We find that while the data is completely uninformative about the kick magnitude, it contains information about its direction.

First, we find that the kick forms an angle $\theta_{KN} = 37^{+15}_{-12}$ deg with the LOS. We find that removing any combination of HMs and precession (green, red, magenta) leads to less informative or biased posteriors.

Second, the prior for θ_{KL} is symmetric around 90 deg (*i.e.*, with respect to the orbital plane) with peaks at $\simeq 20$ and 160 deg. This reflects the well-known fact that precessing sources preferentially lead to kicks out of the orbital plane [13, 16, 72], but with no preference for shooting the final BH up or down, *i.e.*, with a positive or negative projection of the kick onto \mathbf{L} . We find that most of the support shifts to the “upper” branch peaking at $\theta_{KL} \sim 25$ deg (*i.e.* 65 deg off the orbital plane) with a posterior probability 2.5 larger than the prior one. Again, removing HMs leads to a less informative posterior that, in particular, barely distinguishes between the “upper” and “lower” branches. As expected, removing precession constrains the kick to the orbital plane.

Finally, we obtain an informative posterior for ϕ_{KN}^{-100M} yielding $\phi_{KN}^{-100M} = 46^{+32}_{-41}$ deg. Similar to Fig. 3, removing both HMs and precession (green) yields a completely uninformative posterior while, if precession is included, a little information is retrieved thanks to the asymmetry between the $(2, \pm 2)$ modes (blue). Finally, we note that our analysis ignoring precession but including HMs (orange) yields a posterior consistent with that including both effects. We understand this is consistent with the fact that no evidence for orbital precession has been found for GW190412 [56].

IV. CONCLUSIONS

Gravitational recoil is a strong-gravity effect of paramount importance in many astrophysical scenarios. Estimates of kick magnitudes [38] are crucial to understand the retention probability of BHs in their environments and, therefore, their ability to build hierarchical formation channels that can drive the formation of intermediate and supermassive BHs [18]. BHs recoiling through dense environments like Active Galactic Nuclei (AGN) can yield counterpart electromagnetic flares to

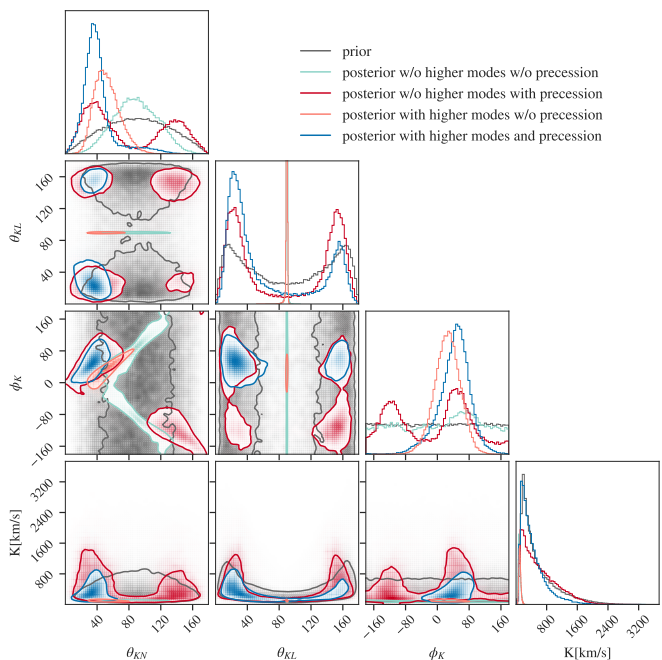


FIG. 4. **Magnitude and direction of the GW190412 recoil.** The side panels show the one-dimensional posterior distribution for the magnitude of the kick of GW190412, together with those for the angles it forms with the line-of-sight θ_{KN} , the orbital plane θ_{KL}^{-100M} , and the projection of the formed onto the latter ϕ_{KN}^{-100M} . The orbital plane is defined at a reference time $t_{\text{ref}} = -100 M$ before merger. The inner panels show the corresponding 2-dimensional 90% credible regions. We show in grey the corresponding priors.

GW signals [73], as those recently proposed in [74, 75]. If real, such multi-messenger observations can enable, *e.g.*, independent estimates of the Hubble constant [76, 77]. Since the properties and observability of the flare depend on the direction of the kick w.r.t. both the host AGN and the observer [75], obtaining such information from the GW side can help to assess the plausibility of the flare as a true counterpart and as a probe of the AGN properties. For instance, if the kick is directed away from the observer, the corresponding flare would most likely be obscured by the optically thick AGN disk. While there is no candidate electromagnetic counterpart to GW190412, we foresee the usage of the recoil direction to assess the plausibility of future candidates.

We stress that our measurement requires an estimate of the *physically meaningful* azimuthal angle ϕ_N of the observer around the source – misleadingly known as “coalescence phase” – that can be compared to kick azimuthal angle ϕ_K . We hope that as gravitational-wave detectors and search techniques improve their respective sensitivities, and the number of events with rich HMs increases, this will become common practice in future gravitational-wave catalogues.

ACKNOWLEDGEMENTS

We thank Nicolas Sanchis-Gual, Barry McKernan, Saavik Ford and Angela Borchers for their comments on the manuscript. We thank Sergei Ossokine and Nathan Johnson-McDaniel for their advice to perform parameter estimation at a given reference time t_{ref} . We also thank Vijay Varma for discussions on the importance of this choice. The analysed data and the corresponding power spectral densities are publicly available at the online Gravitational Wave Open Science Center [78]. JCB is supported by a fellowship from “la Caixa” Foundation (ID100010434) and from the European Union’s

Horizon2020 research and innovation programme under the Marie Skłodowska-Curie grant agreement No 847648. The fellowship code is LCF/BQ/PI20/11760016. KC acknowledges the MHRD, Government of India, for the fellowship support. We acknowledge the use of IUCAA LDG cluster Sarathi for the computational/numerical work. The authors acknowledge computational resources provided by the CIT cluster of the LIGO Laboratory and supported by National Science Foundation Grants PHY-0757058 and PHY0823459, and the support of the NSF CIT cluster for the provision of computational resources for our parameter inference runs. This material is based upon work supported by NSF’s LIGO Laboratory which is a major facility fully funded by the National Science Foundation. This manuscript has LIGO DCC number P2200332.

-
- [1] C. W. Misner, K. S. Thorne, and J. A. Wheeler, *Gravitation* (W. H. Freeman, San Francisco, 1973).
- [2] K. S. Thorne, *Rev. Mod. Phys.* **52**, 299 (1980).
- [3] M. J. Fitchett, *Mon. Not. Roy. Astron. Soc.* **203**, 1049 (1983).
- [4] M. Maggiore, *Gravitational Waves: Volume 1: Theory and Experiments*, Gravitational Waves (OUP Oxford, 2008).
- [5] J. A. Gonzalez, U. Sperhake, B. Bruegmann, M. Hannam, and S. Husa, *Phys. Rev. Lett.* **98**, 091101 (2007), arXiv:gr-qc/0610154 [gr-qc].
- [6] F. Herrmann, I. Hinder, D. Shoemaker, P. Laguna, and R. A. Matzner, *Astrophys. J.* **661**, 430 (2007), arXiv:gr-qc/0701143 [GR-QC].
- [7] M. Koppitz, D. Pollney, C. Reisswig, L. Rezzolla, J. Thornburg, *et al.*, *Phys. Rev. Lett.* **99**, 041102 (2007), arXiv:gr-qc/0701163 [GR-QC].
- [8] P. A. Sundararajan, G. Khanna, and S. A. Hughes, *Phys. Rev. D* **81**, 104009 (2010), arXiv:1003.0485 [gr-qc].
- [9] C. O. Lousto and Y. Zlochower, *Phys. Rev. Lett.* **107**, 231102 (2011), arXiv:1108.2009 [gr-qc].
- [10] J. Calderón Bustillo, J. A. Clark, P. Laguna, and D. Shoemaker, *Phys. Rev. Lett.* **121**, 191102 (2018), arXiv:1806.11160 [gr-qc].
- [11] M. Campanelli, C. O. Lousto, Y. Zlochower, and D. Merritt, *Phys. Rev. Lett.* **98**, 231102 (2007), arXiv:gr-qc/0702133.
- [12] J. A. Gonzalez, M. D. Hannam, U. Sperhake, B. Bruegmann, and S. Husa, *Phys. Rev. Lett.* **98**, 231101 (2007), arXiv:gr-qc/0702052.
- [13] B. Bruegmann, J. A. Gonzalez, M. Hannam, S. Husa, and U. Sperhake, *Phys. Rev. D* **77**, 124047 (2008), arXiv:0707.0135 [gr-qc].
- [14] J. Healy, F. Herrmann, I. Hinder, D. M. Shoemaker, P. Laguna, and R. A. Matzner, *Phys. Rev. Lett.* **102**, 041101 (2009), arXiv:0807.3292 [gr-qc].
- [15] U. Sperhake, B. Bruegmann, D. Mueller, and C. F. Sopuerta, (2010), arXiv:1012.3173 [gr-qc].
- [16] C. O. Lousto and Y. Zlochower, *Phys. Rev. D* **87**, 084027 (2013), arXiv:1211.7099 [gr-qc].
- [17] C. O. Lousto, Y. Zlochower, M. Dotti, and M. Volonteri, *Physical Review D* **85** (2012), 10.1103/physrevd.85.084015.
- [18] D. Gerosa and M. Fishbach, *Nature Astronomy* **5**, 749 (2021), arXiv:2105.03439 [astro-ph.HE].
- [19] M. Volonteri, F. Haardt, and P. Madau, *The Astrophysical Journal* **582**, 559 (2003).
- [20] M. Volonteri, *The Astronomy and Astrophysics Review* **18**, 279 (2010).
- [21] Y. Sakurai, N. Yoshida, M. S. Fujii, and S. Hirano, *Monthly Notices of the Royal Astronomical Society* **472**, 1677 (2017).
- [22] J. Aasi *et al.* (LIGO Scientific), *Class. Quant. Grav.* **32**, 074001 (2015), arXiv:1411.4547 [gr-qc].
- [23] F. Acernese *et al.* (VIRGO), *Class. Quant. Grav.* **32**, 024001 (2015), arXiv:1408.3978 [gr-qc].
- [24] R. Abbott *et al.* (LIGO Scientific, Virgo), *Astrophys. J. Lett.* **900**, L13 (2020), arXiv:2009.01190 [astro-ph.HE].
- [25] V. Varma, S. Biscoveanu, T. Islam, F. H. Shaik, C.-J. Haster, M. Isi, W. M. Farr, S. E. Field, and S. Vitale, “Evidence of large recoil velocity from a black hole merger signal,” (2022), arXiv:2201.01302.
- [26] V. Varma, M. Isi, and S. Biscoveanu, *Physical Review Letters* **124** (2020), 10.1103/physrevlett.124.101104.
- [27] M. Pürrer, M. Hannam, and F. Ohme, *Phys. Rev. D* **93**, 084042 (2016), arXiv:1512.04955 [gr-qc].
- [28] S. Biscoveanu, M. Isi, V. Varma, and S. Vitale, *Phys. Rev. D* **104**, 103018 (2021), arXiv:2106.06492 [gr-qc].
- [29] B. P. Abbott *et al.* (LIGO Scientific, Virgo), *Phys. Rev. X* **9**, 031040 (2019), arXiv:1811.12907 [astro-ph.HE].
- [30] A. H. Nitz, C. Capano, A. B. Nielsen, S. Reyes, R. White, D. A. Brown, and B. Krishnan, *Astrophys. J.* **872**, 195 (2019), arXiv:1811.01921 [gr-qc].
- [31] T. Venumadhav, B. Zackay, J. Roulet, L. Dai, and M. Zaldarriaga, *Phys. Rev. D* **101**, 083030 (2020), arXiv:1904.07214 [astro-ph.HE].
- [32] A. H. Nitz, T. Dent, G. S. Davies, S. Kumar, C. D. Capano, I. Harry, S. Mozzon, L. Nuttall, A. Lundgren, and M. Tápai, *Astrophys. J.* **891**, 123 (2020), arXiv:1910.05331 [astro-ph.HE].
- [33] R. Abbott *et al.* (LIGO Scientific, Virgo), *Phys. Rev. X* **11**, 021053 (2021), arXiv:2010.14527 [gr-qc].
- [34] R. Abbott *et al.* (LIGO Scientific, VIRGO, KAGRA), (2021), arXiv:2111.03606 [gr-qc].

- [35] A. H. Nitz, C. D. Capano, S. Kumar, Y.-F. Wang, S. Kastha, M. Schäfer, R. Dhurkunde, and M. Cabero, *Astrophys. J.* **922**, 76 (2021), arXiv:2105.09151 [astro-ph.HE].
- [36] A. H. Nitz, S. Kumar, Y.-F. Wang, S. Kastha, S. Wu, M. Schäfer, R. Dhurkunde, and C. D. Capano, (2021), arXiv:2112.06878 [astro-ph.HE].
- [37] S. Olsen, T. Venumadhav, J. Mushkin, J. Roulet, B. Zackay, and M. Zaldarriaga, *Phys. Rev. D* **106**, 043009 (2022), arXiv:2201.02252 [astro-ph.HE].
- [38] P. Mahapatra, A. Gupta, M. Favata, K. G. Arun, and B. S. Sathyaprakash, *The Astrophysical Journal Letters* **918**, L31 (2021).
- [39] J. N. Goldberg, A. J. MacFarlane, E. T. Newman, F. Rohrlich, and E. C. G. Sudarshan, *J. Math. Phys.* **8**, 2155 (1967).
- [40] L. Blanchet, *Living Rev. Rel.* **17**, 2 (2014), arXiv:1310.1528 [gr-qc].
- [41] LIGO Scientific Collaboration, “LIGO Algorithm Library - LALSuite,” free software (GPL) (2018).
- [42] P. Schmidt, I. W. Harry, and H. P. Pfeiffer, (2017), arXiv:1703.01076 [gr-qc].
- [43] T. A. Apostolatos, C. Cutler, G. J. Sussman, and K. S. Thorne, *Phys. Rev. D* **49**, 6274 (1994).
- [44] J. Calderón Bustillo, C. Evans, J. A. Clark, G. Kim, P. Laguna, and D. Shoemaker, *Communications Physics* **3**, 176 (2020), arXiv:1906.01153 [gr-qc].
- [45] I. Harry, S. Privitera, A. Bohé, and A. Buonanno, *Phys. Rev. D* **94**, 024012 (2016), arXiv:1603.02444 [gr-qc].
- [46] I. Harry, J. Calderón Bustillo, and A. Nitz, *Phys. Rev. D* **97**, 023004 (2018), arXiv:1709.09181 [gr-qc].
- [47] C. Capano, Y. Pan, and A. Buonanno, *Phys. Rev. D* **89**, 102003 (2014), arXiv:1311.1286 [gr-qc].
- [48] J. C. Bustillo, A. Bohé, S. Husa, A. M. Sintes, M. Hannam, *et al.*, (2015), arXiv:1501.00918 [gr-qc].
- [49] J. Calderón Bustillo, P. Laguna, and D. Shoemaker, *Phys. Rev. D* **95**, 104038 (2017), arXiv:1612.02340 [gr-qc].
- [50] J. Calderón Bustillo, F. Salemi, T. Dal Canton, and K. P. Jani, *Phys. Rev. D* **97**, 024016 (2018), arXiv:1711.02009 [gr-qc].
- [51] K. Chandra, V. Gayathri, J. C. Bustillo, and A. Pai, *Phys. Rev. D* **102**, 044035 (2020), arXiv:2002.10666 [astro-ph.CO].
- [52] K. Chandra, J. Calderón Bustillo, A. Pai, and I. Harry, (2022), arXiv:2207.01654 [gr-qc].
- [53] R. Abbott and Others, “GWTC-3: Compact binary coalescences observed by LIGO and virgo during the second part of the third observing run,” (2021), arXiv:2111.03606.
- [54] M. Hannam, C. Hoy, J. E. Thompson, S. Fairhurst, V. Raymond, M. Colleoni, D. Davis, H. Estellés, C.-J. Haster, A. Helmling-Cornell, S. Husa, D. Keitel, T. J. Massinger, A. Menéndez-Vázquez, K. Mogushi, S. Ossokine, E. Payne, G. Pratten, I. Romero-Shaw, J. Sadiq, P. Schmidt, R. Tenorio, R. Udall, J. Veitch, D. Williams, A. B. Yelikar, and A. Zimmerman, *Nature* (2022), 10.1038/s41586-022-05212-z.
- [55] E. Payne, S. Hourihane, J. Golomb, R. Udall, D. Davis, and K. Chatziioannou, “The curious case of gw200129: interplay between spin-precession inference and data-quality issues,” (2022), arXiv:2206.11932.
- [56] R. Abbott *et al.*, *Physical Review D* **102** (2020), 10.1103/physrevd.102.043015.
- [57] S. Roy, A. S. Sengupta, and K. Arun, *Physical Review D* **103** (2021), 10.1103/physrevd.103.064012.
- [58] R. J. E. Smith, G. Ashton, A. Vajpeyi, and C. Talbot, *Mon. Not. Roy. Astron. Soc.* **498**, 4492 (2020), arXiv:1909.11873 [gr-qc].
- [59] V. Varma, S. E. Field, M. A. Scheel, J. Blackman, D. Gerosa, L. C. Stein, L. E. Kidder, and H. P. Pfeiffer, *Physical Review Research* **1** (2019), 10.1103/physrevresearch.1.033015.
- [60] G. Pratten *et al.*, *Phys. Rev. D* **103**, 104056 (2021), arXiv:2004.06503 [gr-qc].
- [61] S. Ossokine *et al.*, *Phys. Rev. D* **102**, 044055 (2020), arXiv:2004.09442 [gr-qc].
- [62] Y. Pan, A. Buonanno, A. Taracchini, L. E. Kidder, A. H. Mroue, H. P. Pfeiffer, M. A. Scheel, and B. Szilágyi, *Phys. Rev. D* **89**, 084006 (2014), arXiv:1307.6232 [gr-qc].
- [63] S. Babak, A. Taracchini, and A. Buonanno, *Phys. Rev. D* **95**, 024010 (2017), arXiv:1607.05661 [gr-qc].
- [64] P. Schmidt, M. Hannam, and S. Husa, *Phys. Rev. D* **86**, 104063 (2012), arXiv:1207.3088 [gr-qc].
- [65] M. Hannam, P. Schmidt, A. Bohé, L. Haegel, S. Husa, F. Ohme, G. Pratten, and M. Pürrer, *Phys. Rev. Lett.* **113**, 151101 (2014), arXiv:1308.3271 [gr-qc].
- [66] A. Borchers and F. Ohme, “Inconsistent black hole kick estimates from gravitational-wave models,” (2022), arXiv:2207.13531.
- [67] V. Varma, M. Isi, S. Biscoveanu, W. M. Farr, and S. Vitale, *Physical Review D* **105** (2022), 10.1103/physrevd.105.024045.
- [68] J. Calderón Bustillo, S. Husa, A. M. Sintes, and M. Pürrer, *Phys. Rev. D* **93**, 084019 (2016), arXiv:1511.02060 [gr-qc].
- [69] V. Varma, D. Gerosa, L. C. Stein, F. Hébert, and H. Zhang, *Physical Review Letters* **122** (2019), 10.1103/physrevlett.122.011101.
- [70] J. S. Speagle, *Monthly Notices of the Royal Astronomical Society* **493**, 3132 (2020).
- [71] D. Gerosa and C. J. Moore, *Phys. Rev. Lett.* **117**, 011101 (2016), arXiv:1606.04226 [gr-qc].
- [72] V. Varma, D. Gerosa, L. C. Stein, F. Hébert, and H. Zhang, *Physical Review Letters* **122** (2019), 10.1103/physrevlett.122.011101.
- [73] B. McKernan, K. E. S. Ford, I. Bartos, M. J. Graham, W. Lyra, S. Marka, Z. Marka, N. P. Ross, D. Stern, and Y. Yang, *Astrophysical Journal Letters* **884**, L50 (2019), arXiv:1907.03746 [astro-ph.HE].
- [74] M. Graham, K. Ford, B. McKernan, N. Ross, D. Stern, K. Burdge, M. Coughlin, S. Djorgovski, A. Drake, D. Duev, M. Kasliwal, A. Mahabal, S. van Velzen, J. Belecki, E. Bellm, R. Burruss, S. Cenko, V. Cunningham, G. Helou, S. Kulkarni, F. Masci, T. Prince, D. Reiley, H. Rodriguez, B. Rusholme, R. Smith, and M. Soumagnac, *Physical Review Letters* **124** (2020), 10.1103/physrevlett.124.251102.
- [75] M. J. Graham, B. McKernan, K. E. S. Ford, D. Stern, S. G. Djorgovski, M. Coughlin, K. B. Burdge, E. C. Bellm, G. Helou, A. A. Mahabal, F. J. Masci, J. Pridum, P. Rosnet, and B. Rusholme, “A light in the dark: searching for electromagnetic counterparts to black hole-black hole mergers in ligo/virgo o3 with the zwicky transient facility,” (2022), arXiv:2209.13004.
- [76] S. Mukherjee, A. Ghosh, M. J. Graham, C. Karathanasis, M. M. Kasliwal, I. M. Hernandez, S. M. Nissanke, A. Silvestri, and B. D. Wandelt, “First measurement

of the hubble parameter from bright binary black hole gw190521,” (2020), arXiv:2009.14199.

[77] H.-Y. Chen, C.-J. Haster, S. Vitale, W. M. Farr, and M. Isi, “A standard siren cosmological measurement

from the potential GW190521 electromagnetic counterpart ZTF19abannhr,” (2020), arXiv:2009.14057.

[78] Abbott *et al.*, “Gravitational wave open science center strain data release for GW190521, LIGO open science center,” (2020).